

Tough Polylactide Graft Copolymers

Grayce Theryo,[‡] Feng Jing,[†] Louis M. Pitet,[†] and Marc A. Hillmyer^{*†}

[†]Department of Chemistry and [‡]Department of Chemical Engineering and Materials Science, University of Minnesota, Minneapolis, Minnesota 55455-0431

Received May 24, 2010

Revised Manuscript Received August 3, 2010

Polylactide (PLA) is an intriguing polymer from both a biomedical and a sustainable perspective due to its biorenewable origins and benign degradation products.^{1,2} However, the applications of PLA are currently limited by its brittle nature.³ General strategies for polystyrene toughening (e.g., approaches based on polystyrene–polybutadiene block polymers and high impact polystyrene) have inspired a great deal of effort toward increasing the ductility of PLA through the introduction of a rubbery (i.e., low glass transition temperature, low modulus) phase in blends and block copolymers.^{3–10} The rubbery component provides supplementary energy dissipation mechanisms during deformation and thus improves toughness (or ductility).¹¹ To achieve toughening without compromising other mechanical responses, the rubber content should be minimized. For example, high rubber content typically reduces the elastic modulus and (yield) strength of a composite material.^{12,13}

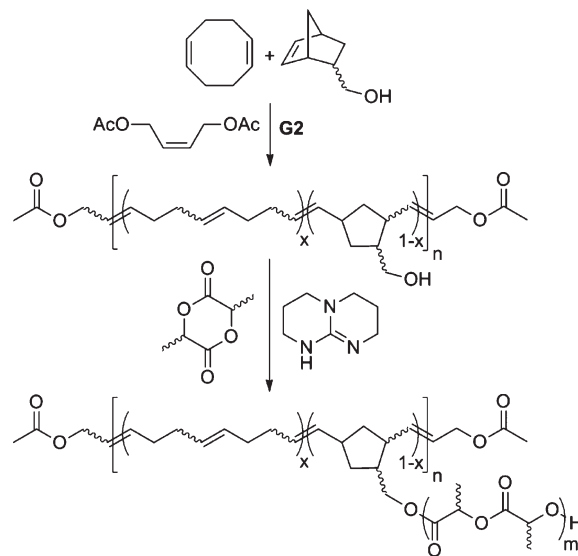
Syntheses of block copolymers containing PLA for modified mechanical behavior have been reported in the literature, but most typically employ a linear architecture with less than about 50 wt % PLA.^{14–16} In the few reported cases of PLA block copolymers containing predominantly PLA, compositions of greater than 90 wt % PLA have rarely been explored.¹⁷ Grijpma and co-workers were able to synthesize a star-block copolymer of poly(trimethylene carbonate) [PTMC] and polylactide containing 6 wt % PTMC.¹⁸ However, the resulting material showed a 15% decrease in tensile yield strength and no increase in ductility when compared with polylactide. To the best of our knowledge, there are no reports of PLA block copolymers containing less than 10 wt % rubber that exhibit improved ductility relative to PLA homopolymer.

Motivated by previous reports, we hypothesize that the synthesis and development of PLA graft copolymers may well provide materials with enhanced toughness.^{19–23} To this end, we recently described the synthesis of a bifunctional monomer consisting of a lactone substituted with a norbornene moiety.²⁴ Ring-opening metathesis polymerization (ROMP) of the bifunctional monomer and 1,5-cyclooctadiene yielded a rubbery macromolecule with pendant lactones. Subsequent ring-opening transesterification polymerization (ROTEP) of DL-lactide in the presence of the rubbery “backbone” provided mixtures composed of polylactide graft copolymer and homopolymer poly(DL-lactide) [PLA]. At 20 wt % rubber, the composite material exhibited significantly enhanced tensile toughness (8×) as compared to a model PLA homopolymer.

Inspired by that study, we now introduce a simplified synthetic approach for the facile synthesis of polylactide graft copolymers (Scheme 1) utilizing both ROMP and ROTEP.^{17,25–28}

First, a rubbery backbone is synthesized by ring-opening metathesis copolymerization of commercially available 1,5-cyclooctadiene (C) and 5-norbornene-2-methanol (N) catalyzed by the second-generation Grubbs’ catalyst (G2).^{17,29} A chain transfer agent (CTA), *cis*-1,4-diacetoxy-2-butene, is used to control the degree of polymerization of the copolymer.³⁰ The resulting polymer, poly(1,5-cyclooctadiene-*co*-5-norbornene-2-methanol) [PCN], has a low glass transition temperature ($T_g \approx -80^\circ\text{C}$) and statistically distributed pendant primary hydroxyl groups capable of initiating the ROTEP of lactide.^{31–34} The average number of grafts per chain and spacing between grafts can be controlled through the comonomer ratio and CTA concentration. ROTEP of DL-lactide (L) [a racemic mixture of the D- and L-stereoisomers] from the PCN macroinitiator catalyzed by 1,5,7-triazabicyclo[4.4.0]dec-5-ene (TBD)^{35,36} provides the desired graft copolymer, poly(1,5-cyclooctadiene-*co*-5-norbornene-2-methanol-*graft*-DL-lactide) [PCNL] (Scheme 1). Although interesting, the effect of PLA crystallinity was not considered in this initial study.

Scheme 1. PLA Graft Copolymer Synthesis



In this Communication, we focus on one specific graft copolymer, PCNL-332-10.9-95, where the numbers respectively designate the number-average degree of polymerization of the 1,5-cyclooctadiene in the PCN backbone, average number of grafts per chain, and weight percent of PLA in the copolymer as determined by nuclear magnetic resonance (NMR) spectroscopy. The theoretical molecular weight of each PLA graft is 65.0 kg/mol. A comparison of the ¹H NMR signals (Figure S2) from the PLA initiation sites along the PCN backbone (the methylene adjacent to the cyclopentane ring in the backbone) and the terminating end groups (the terminal methine proton of the PLA chains) reveals a slight excess of the terminal methine proton (ca. 19 mol %), suggesting the graft copolymer may contain a small portion of PLA homopolymer from adventitious initiation.³⁷ Assuming the molar masses of the free and grafted PLA chain are equal, we calculate the sample as having ~18 wt % PLA homopolymer. The calculated number-average molecular weight (M_n) of all the PLA chains (free and grafted) in the system is 57 kg/mol. On the basis of the molar mass of the PCN backbone, the estimated PLA arm length, and the average number of arms per backbone,

^{*}To whom correspondence should be addressed. E-mail: hillmyer@umn.edu.

we estimate an M_n for PCNL-332-10.9-95 of 659 kg/mol. For comparative purposes, we also prepared a PLA homopolymer sample ($M_n = 59.0$ kg/mol, NMR spectroscopy) initiated by benzyl alcohol using TBD. Size exclusion chromatography (SEC) data for the macroinitiator (Figure 1a), PCN-332-10.9, shows a relatively symmetric, monomodal peak ($M_n = 55.6$ kg/mol, PDI = 1.69, PS standards). PCNL-332-10.9-95 (Figure 1b) elutes at a smaller retention volume than the macroinitiator, indicating successful grafting of PLA from the macroinitiator, but exhibits both high and low molecular weight shoulders ($M_n = 305$ kg/mol, PDI = 2.34, PS standards³⁸). Comparison of the SEC traces for the macroinitiator, graft copolymer, and PLA control (Figure 1c; $M_n = 94$ kg/mol, PDI = 1.88, PS standards) suggests that the low molecular weight shoulder may arise from unfunctionalized backbone chains, PLA homopolymer, or both. The origin of the high molecular weight shoulder of PCNL-332-10.9-95 is currently under investigation.

The morphology adopted by PCNL-332-10.9-95 is important based upon the well-established impact of microphase separation on ductility in rubbery–glassy composites.³⁹ The PCNL-332-10.9-95 graft copolymer presumably lies near the order–disorder phase boundary based on the large compositional asymmetry (95 wt % PLA).^{40,41} However, the anticipated high degree of immiscibility between PLA and the aliphatic PCN backbone^{17,41} combined with an effectively large conformational asymmetry between the PLA grafts and the PCN backbone both favor microphase separation.²⁰ Differential scanning calorimetry (DSC) [Figure S3] of PCN-332-10.9 revealed a T_g of -81 °C and a broad set of endothermic melting transitions between about -10 and 50 °C due to the semicrystalline nature of the poly-(1,5-cyclooctadiene). After grafting of PLA onto the macroinitiator, only a very weak melting transition was observed (centered near 20 °C). The PLA T_g in PCNL-332-10.9-95 was apparent at 57 °C, a value nearly identical to that in the PLA control sample and consistent with microphase separation; the T_g of the rubbery backbone in PCNL-332-10.9-95 was not observable.

Small-angle X-ray scattering (SAXS) of PCNL-332-10.9-95 showed a single peak in the one-dimensional profile of intensity versus spatial frequency (Figure S4), suggesting a microphase-separated structure with a principal domain spacing of ~ 32 nm. Transmission electron microscopy (TEM) of thin sections of PCNL-332-10.9-95 (stained with OsO_4) revealed a phase-separated morphology consisting of spheroidal domains rich in poly-(1,5-cyclooctadiene) [the double bonds in the PCN backbone being stained by OsO_4] surrounded by a matrix of PLA (Figure 2). The thickness of the ultramicrotomed sections (~ 70 nm) results in overlapping rubber domains and the appearance that more than 5% of the imaged area is stained. Although the TEM image is a two-dimensional projection of a three-dimensional sample, the approximate domain spacing (~ 30 nm) supports the results from SAXS. Both the PCNL-332-10.9-95 and PLA control sample were optically transparent (Figure 3a,c).

The mechanical behavior of PCNL-332-10.9-95 was characterized by tensile testing of compression-molded samples.⁴² Mechanical properties of the graft copolymer were compared to those of the PLA control. The PLA control (Figure 3a,b) failed catastrophically after a relatively small amount of deformation without neck formation and only slight stress whitening, characteristic of a brittle material. On the contrary, the graft copolymer exhibited stress whitening, neck formation, and cold drawing, resulting in extensive elongation (Figure 3c,d). Representative engineering stress–strain curves for both materials are shown in Figure 4. On average, the PLA control elongated to $13 \pm 4\%$ before failure, similar to a reported literature value for amorphous poly(L-lactide).⁴³ In contrast, PCNL-332-10.9-95 exhibited an average ultimate elongation of $238 \pm 43\%$, a 1700% increase relative to PLA. Furthermore, the average tensile

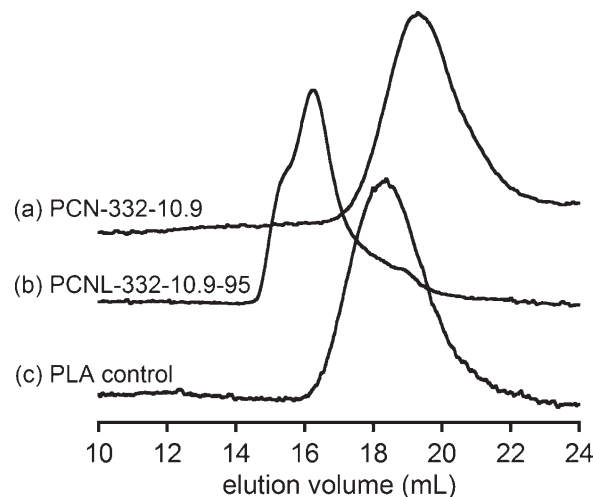


Figure 1. Size-exclusion chromatograms of (a) the PCN-332-10.9 macroinitiator, (b) the PCNL-332-10.9-95 graft copolymer, and (c) the PLA control sample.

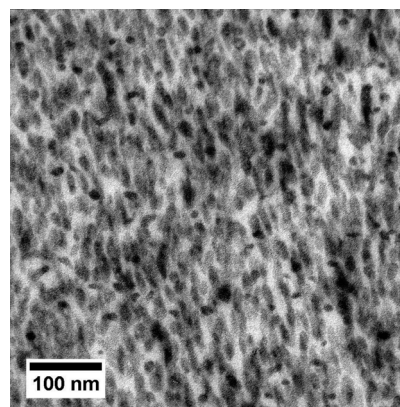


Figure 2. Transmission electron micrograph of PCNL-332-10.9-95 reveals a microphase-separated morphology (OsO_4 staining; ~ 70 nm thickness).

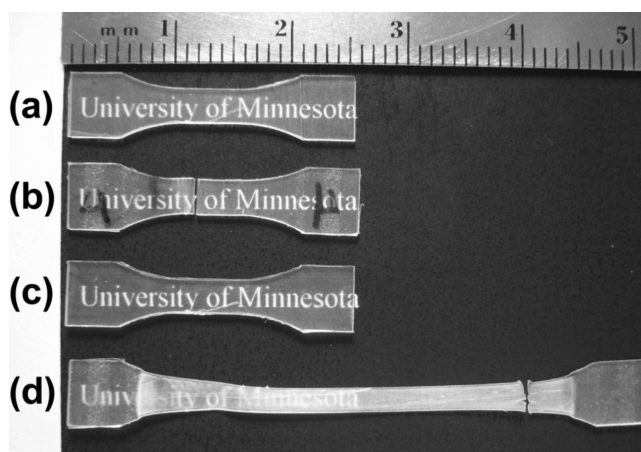


Figure 3. Representative tensile bars illustrate the PLA control (a) before and (b) after tensile testing. The significant increase in ultimate elongation, stress whitening, and necking of PCNL-332-10.9-95 (d) after testing, relative to (c) before testing, is readily apparent.

modulus, E , and yield strength, σ_y , of the graft copolymer ($E = 1.86 \pm 0.09$ GPa, $\sigma_y = 64.8 \pm 2.0$ MPa) were only slightly lower than the PLA control ($E = 2.03 \pm 0.07$ GPa, $\sigma_y = 67.9 \pm 1.3$ MPa). Overall, the tensile toughness of PCNL-332-10.9-95 was

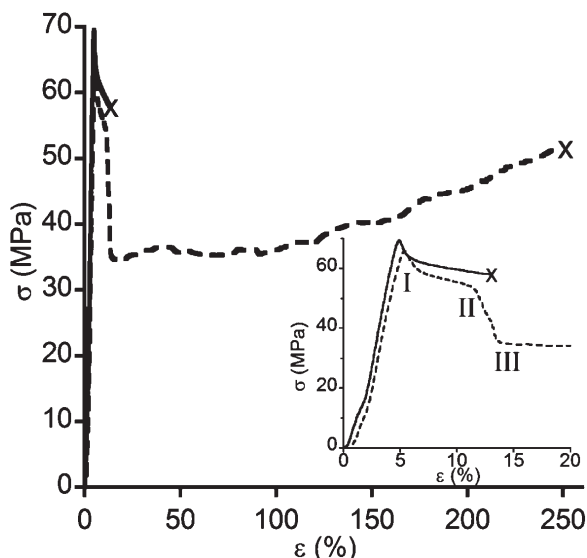


Figure 4. Representative engineering stress–strain curves illustrate the increase in ultimate elongation of PCNL-332-10.9-95 (---) relative to PLA (—). The failure points are denoted by the \times 's. The small strain limit is shown in the inset highlighting the similar tensile modulus and yield strength of the two materials.

remarkably 14 times larger than the PLA control sample ($95 \pm 23 \text{ MJ/m}^3$ vs $7 \pm 2 \text{ MJ/m}^3$).⁴⁴ Notably, the graft copolymer exhibited two yield points, the first at $\sim 6\%$ strain (I) and the second, corresponding to the onset of neck formation, at $\sim 12\%$ strain (II) before the start of cold drawing at nearly constant stress (III) as seen in the inset of Figure 4.

Plastic deformation in rubber-toughened glassy polymers can occur through a number of mechanisms including crazing, cavitation of the rubber phase, and shear yielding.⁴⁵ Whitening of the gage region was observed in PCNL-332-10.9-95 before neck formation. Additionally, some whitening was observed in the PLA homopolymer, and a comparison of the tensile curves reveals similar stress values from about 6–12% strain. As PLA homopolymer is known to deform by a crazing mechanism,⁴³ it is possible that the graft copolymer also deforms from point I to point II (denoted in the Figure 4 inset) by a similar crazing mechanism. When considering the possibility of rubber phase cavitation, theoretical models predict that the critical volume strain required to cause cavitation is inversely proportional to the size of the rubbery domains.^{45,46} Thus, if the small size of the rubber domains in the graft copolymer causes the critical stress for cavitation to be greater than that for an alternative deformation mechanism (e.g., matrix crazing), the matrix phase may yield prior to cavitation. However, Lazzeri and Bucknall have noted that cavitation of the rubber domain may still occur even after initial deformation of the matrix phase provided that strain hardening takes place, resulting in an increase of the true stress.⁴⁷ Consequently, despite their nanoscale dimensions, cavitation of the rubber domains may also play a role in the initial deformation of the graft copolymer. Experimental evidence for cavitation of nanoscale rubber particles in glassy polymer matrices has been reported in the literature, supporting its feasibility.^{13,48,49}

After the initial deformation from point I to point II (Figure 4), a decrease in the engineering stress occurs from point II to point III due to the formation of a neck with reduced cross-sectional area relative to the undeformed gage. At point III, cold drawing begins and the engineering stress remains approximately constant near 35 MPa due to the propagation of the neck through the gage length.¹² The stress then increases up to about 50 MPa as the cold drawing front approaches the grips of the tensile bar before catastrophic failure in the gage takes place. Both neck formation

and cold drawing have been attributed to shear yielding mechanisms¹² and were not observed for homopolymer PLA. The presence of the rubber domains coupled with the graft architecture of the block copolymer has altered the deformation mechanism that occurs in uniaxial extension when compared with homopolymer PLA. The exact role of the rubber phase in the deformation mechanism and the effect of block copolymer architecture and composition are ripe for further investigation.

In summary, a rubber-toughened PLA hybrid material containing only 5 wt % rubber was synthesized using a grafting-from approach. Despite the large compositional asymmetry, a microphase-separated morphology was observed by SAXS and TEM analysis. The large improvement in tensile ductility (without a major loss of strength or rigidity) observed for the graft copolymer relative to PLA demonstrates the potential for an optically transparent and impact-resistant polylactide-based material. We are currently exploring the molecular parameters needed to achieve the improved properties in these materials and their influence on impact performance.

Acknowledgment. This work was supported by the USDA and the U.S. DOE through Grant DE-PS36-06GO96002P. G.T. thanks the University of Minnesota for a graduate student fellowship. Parts of this work were carried out in the Institute of Technology Characterization Facility, University of Minnesota, a member of the NSF-funded Materials Research Facilities Network. SAXS data were acquired at the DuPont–Northwestern–Dow Collaborative Access Team (DND-CAT) located at Sector 5 of the Advanced Photon Source (APS). DND-CAT is supported by E. I. DuPont de Nemours and Co., The Dow Chemical Co., and the State of Illinois. Use of the APS was supported by the U.S. Department of Energy, Office of Science, Office of Basic Energy Sciences, under Contract DE-AC02-06CH11357. The authors thank Dr. Megan L. Robertson for helpful discussions.

Supporting Information Available: Experimental details and supporting NMR, DSC, and SAXS characterization data. This material is available free of charge via the Internet at <http://pubs.acs.org>.

References and Notes

- (1) Williams, C. K.; Hillmyer, M. A. *Polym. Rev.* **2008**, *48*, 1–10.
- (2) Gupta, A. P.; Kumar, V. *Eur. Polym. J.* **2007**, *43*, 4053–4074.
- (3) Anderson, K. S.; Schreck, K. M.; Hillmyer, M. A. *Polym. Rev.* **2008**, *48*, 85–108.
- (4) Anderson, K. S.; Lim, S. H.; Hillmyer, M. A. *J. Appl. Polym. Sci.* **2003**, *89*, 3757–3768.
- (5) Oyama, H. T. *Polymer* **2009**, *50*, 747–751.
- (6) Jiang, L.; Wolcott, M. P.; Zhang, J. *Biomacromolecules* **2006**, *7*, 199–207.
- (7) Jiang, L.; Liu, B.; Zhang, J. *Ind. Eng. Chem. Res.* **2009**, *48*, 7594–7602.
- (8) Bhardwaj, R.; Mohanty, A. K. *Biomacromolecules* **2007**, *8*, 2476–2484.
- (9) Kaneko, H.; Saito, J.; Kawahara, N.; Matsuo, S.; Matsugi, T.; Kashiwa, N. In *Polypropylene-graft-poly(methyl methacrylate) Graft Copolymers: Synthesis and Compatibilization of Polypropylene/Poly(lactide)*; Controlled/Living Radical Polymerization: Progress in ATRP; American Chemical Society: Washington, DC, 2009; Vol. 1023, pp 357–371.
- (10) Liu, H.; Chen, F.; Liu, B.; Estep, G.; Zhang, J. *Macromolecules* **2010**, *43*, 6058–6066.
- (11) Perkins, W. G. *Polym. Eng. Sci.* **1999**, *39*, 2445–2460.
- (12) Haward, R. N.; Young, R. J., Eds. In *The Physics of Glassy Polymers*; Chapman & Hall: London, 1997.
- (13) Jansen, B. J. P.; Rastogi, S.; Meijer, H. E. H.; Lemstra, P. J. *Macromolecules* **2001**, *34*, 3998–4006.
- (14) Frick, E. M.; Zalusky, A. S.; Hillmyer, M. A. *Biomacromolecules* **2003**, *4*, 216–223.
- (15) Cohn, D.; Hotovely-Salomon, A. *Polymer* **2005**, *46*, 2068–2075.
- (16) Wanamaker, C. L.; O'Leary, L. E.; Lynd, N. A.; Hillmyer, M. A.; Tolman, W. B. *Biomacromolecules* **2007**, *8*, 3634–3640.

- (17) Pitet, L. M.; Hillmyer, M. A. *Macromolecules* **2009**, *42*, 3674–3680.
- (18) Grijpma, D. W.; Joziassse, C. A. P.; Pennings, A. J. *Makromol. Chem., Rapid Commun.* **1993**, *14*, 155–161.
- (19) Pae, Y. J. *Appl. Polym. Sci.* **2006**, *99*, 300–308.
- (20) Milner, S. T. *Macromolecules* **1994**, *27*, 2333–2335.
- (21) Xenidou, M.; Beyer, F. L.; Hadjichristidis, N.; Gido, S. P.; Tan, N. B. *Macromolecules* **1998**, *31*, 7659–7667.
- (22) Zhu, Y.; Burgaz, E.; Gido, S. P.; Staudinger, U.; Weidisch, R.; Uhrig, D.; Mays, J. W. *Macromolecules* **2006**, *39*, 4428–4436.
- (23) Adhikari, R.; Michler, G. H. *Prog. Polym. Sci.* **2004**, *29*, 949–986.
- (24) Jing, F.; Hillmyer, M. A. *J. Am. Chem. Soc.* **2008**, *130*, 13826–13827.
- (25) Czelusniak, I.; Khosravi, E.; Kenwright, A. M.; Ansell, C. W. G. *Macromolecules* **2007**, *40*, 1444–1452.
- (26) Oh, S.; Lee, J.; Theato, P.; Char, K. *Chem. Mater.* **2008**, *20*, 6974–6984.
- (27) Wang, Y.; Noga, D. E.; Yoon, K.; Wojtowicz, A. M.; Lin, A. S. P.; Garcia, A. J.; Collard, D. M.; Weck, M. *Adv. Funct. Mater.* **2008**, *18*, 3638–3644.
- (28) Runge, M. B.; Dutta, S.; Bowden, N. B. *Macromolecules* **2006**, *39*, 498–508.
- (29) Bielawski, C. W.; Grubbs, R. H. *Angew. Chem., Int. Ed.* **2000**, *39*, 2903–2906.
- (30) Hillmyer, M. A.; Nguyen, S. T.; Grubbs, R. H. *Macromolecules* **1997**, *30*, 718–721.
- (31) Breitenbach, A.; Kissel, T. *Polymer* **1998**, *39*, 3261–3271.
- (32) Tasaka, F.; Ohya, Y.; Ouchi, T. *Macromolecules* **2001**, *34*, 5494–5500.
- (33) Liu, Y.; Tian, F.; Hu, K. A. *Carbohydr. Res.* **2004**, *339*, 845–851.
- (34) Raynaud, J.; Choquenot, B.; Marie, E.; Dellacherie, E.; Nouvel, C.; Six, J.-L.; Durand, A. *Biomacromolecules* **2008**, *9*, 1014–1021.
- (35) Lohmeijer, B. G. G.; Pratt, R. C.; Leibfarth, F.; Logan, J. W.; Long, D. A.; Dove, A. P.; Nederberg, F.; Choi, J.; Wade, C.; Waymouth, R. M.; Hedrick, J. L. *Macromolecules* **2006**, *39*, 8574–8583.
- (36) Kiesewetter, M. K.; Shin, E. J.; Hedrick, J. L.; Waymouth, R. M. *Macromolecules* **2010**, *43*, 2093–2107.
- (37) The calculated excess is just outside the experimental error of NMR analysis, and thus further analysis is warranted.
- (38) The M_n and PDI determined for the PLA control and PCNL-332-10.9-95 were calculated using a linear extrapolation of the SEC calibration curve.
- (39) Michler, G. H. Micromechanical Mechanisms of Toughness Enhancement in Nanostructured Amorphous and Semicrystalline Polymers. In *Mechanical Properties of Polymers Based on Nanostructure and Morphology*; Michler, G. H., Balta-Calleja, F. J., Eds.; CRC Press, Taylor and Francis Group: Boca Raton, FL, 2005; Vol. 71, pp 248–301.
- (40) Bates, F. S.; Fredrickson, G. H. *Annu. Rev. Phys. Chem.* **1990**, *41*, 525–557.
- (41) Schmidt, S. C.; Hillmyer, M. A. *J. Polym. Sci., Part B: Polym. Phys.* **2002**, *40*, 2364–2376.
- (42) In general, the toughness of a material will depend upon its geometry as well as the mode and rate of loading.¹¹ Impact tests, such as an Izod test, typically characterize resistance to high rates of deformation. A tensile test may also be used to characterize energy dissipation by plastic deformation; however, the rate of loading is relatively slower, and the result will not necessarily be directly related to impact strength.¹¹
- (43) Renouf-Glauser, A. C.; Rose, J.; Farrar, D. F.; Cameron, R. E. *Biomaterials* **2005**, *26*, 5771–5782.
- (44) Tensile toughness was determined from integration of the engineering stress–strain curve. At least four samples were tested to determine the average and standard deviation values.
- (45) Bucknall, C. B. *J. Polym. Sci., Part B: Polym. Phys.* **2007**, *12*, 1399–1409.
- (46) Guild, F.; Kinloch, A.; Taylor, A. *J. Mater. Sci.* **2010**, *14*, 3882–3894.
- (47) Lazzeri, A.; Bucknall, C. B. *Polymer* **1995**, *15*, 2895–2905.
- (48) Jansen, B. J. P.; Rastogi, S.; Meijer, H. E. H.; Lemstra, P. J. *Macromolecules* **2001**, *34*, 4007–4018.
- (49) Liu, J.; Sue, H.; Thompson, Z. J.; Bates, F. S.; Dettloff, M.; Jacob, G.; Verghese, N.; Pham, H. *Macromolecules* **2008**, *41*, 7616–7624.